Extreme Mechanics Letters 15 (2017) 0–5

Contents lists available at ScienceDirect

Extreme Mechanics Letters

journal homepage: www.elsevier.com/locate/eml

Giant non-Schmid effect in NiTi

S. Alkan, Y. Wu, H. Sehitoglu *

Department of Mechanical Science and Engineering, University of Illinois at Urbana–Champaign, 1206 W. Green Street, Urbana, IL 61801, USA

GRAPHICAL ABSTRACT

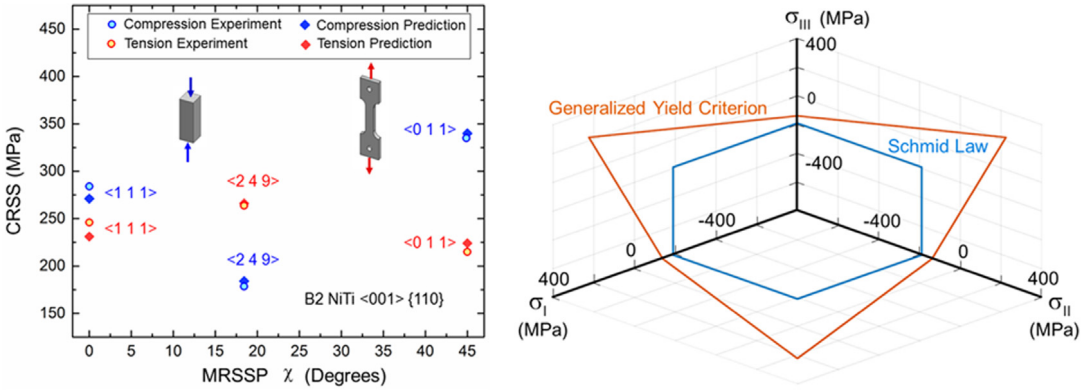

ARTICLE INFO

Article history:
Received 20 March 2017
Received in revised form
18 April 2017
Accepted 9 May 2017
Available online 13 May 2017

ABSTRACT

The work addresses the departure from Schmid law during plasticity of shape memory alloy, NiTi, that has been overlooked despite its cardinal importance. High resolution Digital Image Correlation (DIC) technique is utilized to pinpoint the critical resolved shear stress (CRSS) levels in uniaxial tension and compression experiments. To our knowledge, the non-Schmid behavior of B2 NiTi is characterized for the first time precisely, and the results indicate that the non-glide stresses (both shear and normal character) play a considerable role on yielding. The non-glide stresses affect the core spreading which in turn dictates the changes in CRSS. A generalized yield criterion is proposed to predict the anisotropic experimental response accurately.

1. Introduction

It is well known that dislocation-mediated slip in shape memory alloys (SMAs) considerably modifies their functionality. Slip can be induced during transformation modifying the internal stresses and can create high dislocation densities [1–3], affects the stress and thermal hysteresis [4], changes the transformation strain [5], and the fatigue response [6]. Understanding of slip behavior remains a current [7] and a complex topic [8]. Because the austenite phase is an ordered bcc in most cases, it will not conform to simple Schmid law. The previous treatments of transformation-plasticity will need to be revisited, because non-Schmid yield criteria must be considered. Such a modification is important not only in deformation studies [9] but also in better models for fatigue in NiTi alloys [10]. In this study we establish the form of the non-Schmid law for the most important shape memory material, the near equiatomic NiTi alloy. We provide a background on the non-Schmid phenomenon and then proceed to the experiments and non-Schmid law description for NiTi.

The Schmid law asserts that (i) the plastic flow begins when the resolved shear stress on a possible slip system reaches a "unique"

* Corresponding author.
E-mail address: huseyin@illinois.edu (H. Sehitoglu).

http://dx.doi.org/10.1016/j.eml.2017.05.003
2352-4316/

CRSS value and (ii) the CRSS value is not affected by the other stress components except the one along the Burgers' vector, i.e. glide shear stress [11,12]. The Schmid law is known to hold well for face-centered cubic metals on close packed {111} planes and hexagonal close-packed metals oriented for basal slip [13,14]. However, the glide resistance in the other lattice structures are known to exhibit significant deviations from the Schmid Law [12,15–17]. In case of body centered cubic (bcc) structured materials, such as bcc, and ordered lattices B2, DO_3, $L2_1$, the interplay between the glide and the non-glide stress components, i.e. the non-glide shear and normal stresses acting on the glide plane, results in "non-unique" CRSS levels [17,18]. To that end, the dislocation based plasticity in B2 ordered austenitic NiTi alloy, which is primarily known by its superior superelastic and shape memory properties [3,19,20], could also exhibit a departure from Schmid law. Thus, in this work, we aim to quantify these possible deviations from the Schmid law in B2 NiTi utilizing the uniaxial tension and compression experiments at 293 K.

The stark non-Schmid yielding effects observed in pure bcc metals [21–23] and bcc based intermetallics [24–26], revealed the necessity for the modification of the symmetric yield surfaces utilized in the conventional Schmid Law based crystal plasticity theory [27,28] by introducing the contributions of non-glide stresses at the onset of slip [29–32]. Although considerable effort has been attributed to model the asymmetric "transformation" surfaces in NiTi [20,33,34], no comprehensive study has yet forwarded a modified Schmid law for slip. To that end, a generalized yielding criterion encompassing non-Schmid effects is proposed based on unique experimental measurements in this study.

In this work, we quantify the non-Schmid behavior in B2 ordered NiTi alloy, with 50.8% at. Ni composition, at 293 K and establish a criterion to embrace the deviations from the Schmid law at the onset of slip. To that end, we conducted uniaxial tension and compression experiments on single crystals whose loading axes are oriented along the ⟨111⟩, ⟨249⟩, ⟨011⟩ crystallographic directions (i.e. six cases). To pinpoint the active glide systems and the corresponding CRSS values, the strain fields were tracked by high-resolution, *in-situ* DIC (Digital Image Correlation) technique. Remarkably, our experimental results demonstrate the significant anisotropic yielding behavior of B2 NiTi. As a final step, we constructed a generalized yield criterion accurately reflecting the deviations from the Schmid law based on multi-variable regression.

2. Experimental methods and results

2.1. Experimental methods

Single crystals of 50.8% at. Ni–NiTi, were grown by Bridgman technique in an inert environment. The dog bone tensile samples (net gage section with 8 mm × 3 mm × 1.5 mm) and the compression samples (8 mm × 4 mm × 4 mm) were sectioned using electro-discharge machining. The samples are solution-treated in an inert gas atmosphere following a two-step procedure: (i) for 20 h at 1273 K + water quench and (ii) for 0.5 h at 1203 K + water quench, to produce B2 order. This heat treatment results in transformation temperatures well below 77 K permitting study of plastic slip at 293 K where NiTi is in the stable austenitic regime. Furthermore, post-deformation EBSD analyses are conducted which confirm that the deformation is accommodated only by dislocation mediated slip, not by transformation induced phase change or by deformation twinning. Ruling out possible transformation and deformation twinning is important in devising the correct form of the CRSS modification. The solutionizing treatment also results in no precipitates and ensures the compositional homogeneity.

Table 1
The sample orientations obtained by EBSD analyses are tabulated. The vectors $\boldsymbol{E}_2$ and $\boldsymbol{E}_3$ are directed along the outward normal of the surfaces on which the applied loading acts and the deformation is tracked by the DIC respectively. Their cross product, $\boldsymbol{E}_2 \times \boldsymbol{E}_3$, gives the transverse direction, $\boldsymbol{E}_1$. It is noted that $\boldsymbol{E_1} - \boldsymbol{E_2} - \boldsymbol{E_3}$ triad forms a right-handed orthogonal coordinate frame (also see Fig. 1).

Sample	E_1	E_2
⟨111⟩ tension	$[1\ -2\ -1]/\sqrt{6}$	$[-1\ -1\ 1]/\sqrt{3}$
⟨111⟩ compression	$[1\ 0\ 1]/\sqrt{2}$	$[-1\ -1\ 1]/\sqrt{3}$
⟨249⟩ tension	$[6\ 167\ -70]/\sqrt{32825}$	$[-9\ 2\ 4]/\sqrt{101}$
⟨249⟩ compression	$[6\ 167\ -70]/\sqrt{32825}$	$[-9\ 2\ 4]/\sqrt{101}$
⟨011⟩ tension	$[2\ 1\ 2]/3$	$[-1\ 0\ 1]/\sqrt{2}$
⟨011⟩ compression	$[-2\ -1\ -2]/3$	$[-1\ 0\ 1]/\sqrt{2}$

Table 2
The activated slip systems in B2 NiTi under uniaxial tension and compression are tabulated.

	⟨111⟩	⟨249⟩	⟨011⟩
Tension	$[\bar{1}00](0\bar{1}1)$	$[001](\bar{1}10)$	$[\bar{1}00](011)$
Compression	$[100](0\bar{1}1)$	$[00\bar{1}](\bar{1}10)$	$[100](011)$

Following the treatment, the orientations are confirmed by the Electron Backscatter Diffraction (EBSD) analyses by JEOL 7000 F Scanning Electron Microscope enabling the longitudinal and transverse sample directions known. The specimen orientations are tabulated in Table 1.

The uniaxial tension and compression experiments are conducted in an MTS servo-hydraulic load frame at a strain rate of 5×10^{-5} s^{-1} at 293 K. The sample surfaces are mechanically polished to mirror-finish and a speckle-pattern is deposited on the surface of each sample experimented. The images of the patterned-surface are captured during the experiments by utilizing a CCD camera with a resolution of 3 μm/pix. The deformation is tracked by implementing the DIC analysis with the synchronized stress measurements. The resulting displacement and strain fields are utilized to pinpoint the activation of slip. Slip traces are utilized on all four surfaces of each sample to uniquely determine the active glide system. Such an in-situ measurement of strain is necessary to pinpoint precisely the corresponding stress at onset of slip nucleation. This methodology is a considerable improvement over defining a yield-offset strain based on macroscopic, rather than local, measurements.

2.2. Results of the uniaxial tension and compression experiments

Fig. 1 shows the stress vs. strain curves of the samples oriented along the ⟨111⟩, ⟨249⟩ and ⟨011⟩ crystallographic directions under uniaxial tension and compression. In all of the samples experimented, the active glide system is determined to belong to ⟨001⟩ {110} family as tabulated in Table 2. This trend complies with the reported experimental work and the slip energetics calculations in the literature [35–39].

The variation of CRSS under tension and compression for ⟨001⟩ {110} glide systems are plotted in Fig. 2 using the conventional angle χ which is measured from the reference {110} plane towards the Maximum Resolved Shear Stress Plane (MRSSP) [40]. It is to be noted the symmetry of the B2 lattice structure bounds the angle χ between 0° and 45°. As can be seen, the CRSS values under compression are greater than under tension for the ⟨111⟩ and ⟨011⟩ sample orientations while the reverse behavior is observed in ⟨249⟩ oriented samples. Though the ⟨011⟩ oriented sample is measured to have the greatest glide resistance under compression; the ⟨249⟩ oriented sample exhibits the highest CRSS under tension. An important point to note is that the CRSS values exhibit significant variation under tension and

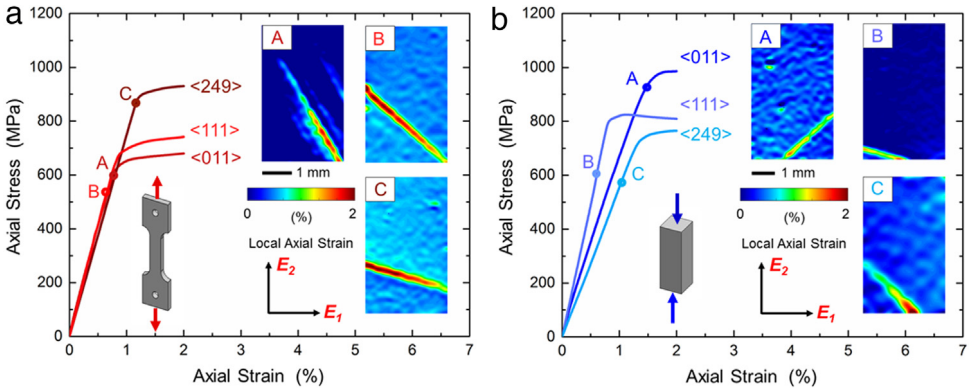

Fig. 1. (a) shows the stress vs. strain curves under uniaxial tension. The points marked as A, B and C on the curves indicate the onset of slip for ⟨011⟩, ⟨111⟩ and ⟨249⟩ orientations. The insets correspond to the axial strain fields generated by DIC at the instant that the slip is detected on the sample surface with outward normal of $\boldsymbol{E}_3$, i.e. equal to $\boldsymbol{E}_1 \times \boldsymbol{E}_2$. (b) shows the stress vs. strain curves under uniaxial compression. Similarly, A, B and C on the curves indicate the onset of slip for ⟨011⟩, ⟨111⟩ and ⟨249⟩ orientations. The insets correspond to the axial strain fields generated by DIC at the instant that the slip is detected on the sample surface with outward normal of $\boldsymbol{E}_3$.

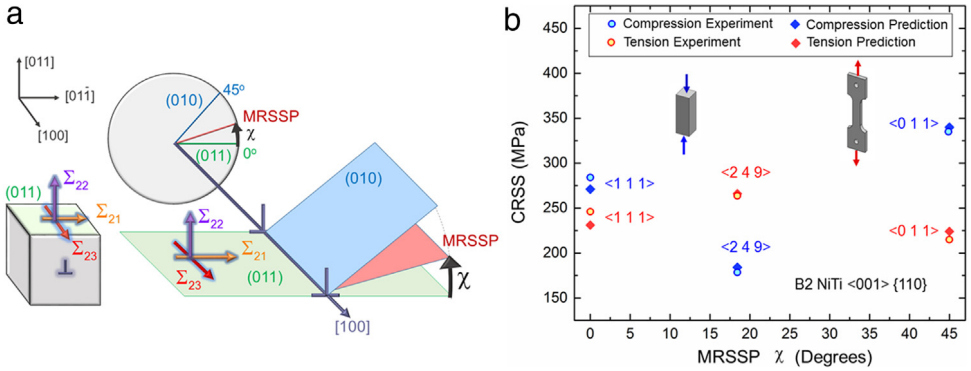

Fig. 2. (a) The χ angle convention is provided with the local stress tensor, $\boldsymbol{\Sigma}$, components on the active glide plane which is (011) along with the [100] Burgers' vector direction in this illustration. In general, the angle χ is defined to traverse from the {110} plane bearing the greatest Σ_{23} towards the MRSSP. (b) The variation of the CRSS values with respect to χ angle are provided for B2 NiTi based on the experiments under uniaxial tension and compression at 293 K (this study). The predicted values from the generalized yield criterion proposed in Eq. (1) are also included for comparison purposes (this study).

compression with a differential of 120 MPa, 85 MPa and 42 MPa for the ⟨011⟩, ⟨249⟩ and ⟨111⟩ sample orientations respectively. Such a differential is rather substantial in ⟨011⟩ case and is above 50% between tension–compression.

2.3. Applied stress components

The results of the uniaxial loading experiments show convincingly that the plastic yielding is not governed by a unique critical value of the glide shear stress. To illustrate this non-unique nature of CRSS values and to quantify the contributions of the other applied stress tensor components, we introduce a right-handed, orthonormal dislocation coordinate frame $\mathbf{e_1} - \mathbf{e_2} - \mathbf{e_3}$ of which the basis vectors $\mathbf{e_2}$ and $\mathbf{e_3}$ are parallel to glide plane normal and the slip vector of the activated slip system respectively. For uniaxial applied stress, the stress tensor, $\boldsymbol{\sigma}$, has a finite σ_{22} component (other components are zeros) in the global specimen coordinate frame of $\boldsymbol{E_1} - \boldsymbol{E_2} - \boldsymbol{E_3}$. The applied stress tensor, $\boldsymbol{\sigma}$, is transformed to the stress tensor in the dislocation frame, $\boldsymbol{\Sigma}$, by an appropriate tensor transformation. As hydrostatic pressure is known to have virtually no significant contribution on dislocation mobility [41], we suggest neglecting its effect and focusing our attention on the deviatoric stress tensor, $\mathbf{S}$, to characterize the role of external loading on the plastic yielding. The deviatoric stress tensor is defined as $\mathbf{S} = \boldsymbol{\Sigma} - p\mathbf{I}$ in which p is equal to 1/3 of the trace of $\boldsymbol{\Sigma}$ and $\mathbf{I}$ is the second order identity tensor [42]. The components of $\mathbf{S}$ are tabulated in Table 3for each sample at the onset of slip.

2.4. The generalized yield criterion

For any ⟨001⟩ {110} family glide system activated in B2 NiTi, the {110} family planes in the slip vector zone are perpendicular to each other. Therefore, the independent components of the applied $\mathbf{S}$ tensor in the orthonormal dislocation frame of $\mathbf{e}_1 - \mathbf{e}_2 - \mathbf{e}_3$ are utilized to introduce a yield condition that can establish the non-Schmid behavior. Based on this rationale, we suggest the following criterion in Eq. (1) for the onset of slip.

$$\tau^*_{cr} = \text{CRSS} + a_1 S_{12} + a_2 S_{22} + a_3 S_{13} + a_4 S_{11}. \tag{1}$$

In Eq. (1), the parameters τ^*_{cr}, a_1, a_2, a_3 and a_4 are material dependent and can be found by a multi-variable linear regression analysis. These parameters are evaluated as displayed in Table 4 conforming to the experimental data presented in Tables 2 and 3. Conventionally, for the Schmid Law, these parameters are equal to zero except τ^*_{cr} which is set equal to a unique CRSS value based on the experimental measurements. On the other hand, as can be seen in Table 4, the multi-variable linear regression of the experimental CRSS values show that the Schmid Law is insufficient to describe the onset of slip in B2 NiTi since a_1, a_2, a_3 and a_4 are of finite magnitude. The negative sign of the coefficients a_1 and a_3 demonstrates that the positive sign shear stresses, S_{21} and S_{13} acting on the {110} planes promote glide resistance, i.e. increase CRSS. Similarly, the tensile normal components S_{11} and S_{22} also elevate the CRSS value.

Table 3
The components of the deviatoric stress tensor, **S**, are tabulated for each sample orientation under tension and compression at the onset of slip. The given expressions are in units of MPa. The CRSS values, i.e. equal to S_{23}, are expressed in bold.

⟨111⟩ tension	⟨249⟩ tension	⟨011⟩ tension
$\mathbf{S}=\begin{bmatrix}-172.7 & 0 & 0\\ 0 & 172.7 & \mathbf{246.0}\\ 0 & 246.0 & 0\end{bmatrix}$	$\mathbf{S}=\begin{bmatrix}-81.7 & -332.9 & -166.4\\ -332.9 & 233.6 & \mathbf{262.8}\\ -166.4 & 262.8 & -151.9\end{bmatrix}$	$\mathbf{S}=\begin{bmatrix}-51.1 & 153.5 & 214.9\\ 153.5 & -51.1 & \mathbf{214.9}\\ 214.9 & 214.9 & 102.2\end{bmatrix}$
⟨111⟩ compression	⟨249⟩ compression	⟨011⟩ compression
$\mathbf{S}=\begin{bmatrix}199.5 & 0 & 0\\ 0 & -199.5 & \mathbf{284.2}\\ 0 & 284.2 & 0\end{bmatrix}$	$\mathbf{S}=\begin{bmatrix}55.3 & -225.3 & 112.6\\ -225.3 & -158.1 & \mathbf{177.9}\\ 112.6 & 177.9 & 102.8\end{bmatrix}$	$\mathbf{S}=\begin{bmatrix}79.7 & 239.2 & -334.9\\ 239.2 & 79.7 & \mathbf{334.9}\\ -334.9 & 334.9 & -159.4\end{bmatrix}$

Table 4
The parameters of the proposed generalized yielding criterion for B2 NiTi in Eq. (1) are tabulated.

τ_{cr}^{*}	a_1	a_2	a_3	a_4
249.2 MPa	−0.11	−0.51	−0.06	−0.62

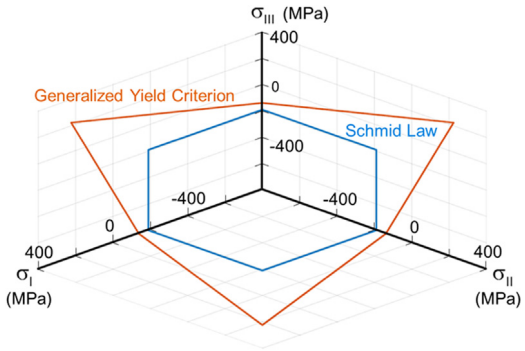

Fig. 3. The yield loci projected on the deviatoric plane in principal stress space for the generalized yield criterion based on Eq. (1) and the conventional Schmid law are shown.

2.5. The yield surface construction

The accurate characterization of the non-Schmid plastic yielding behavior of B2 NiTi for a general applied stress state requires the construction of a convex yield surface which encloses the elastic deformation states. This goal can be achieved by extending the governing methodology utilized under uniaxial loading to the 3-D principal stress space. In this scheme, to span all the possible stress states, the principal stress components are written by introducing the azimuthal angles $\theta([0,\pi])$ and $\phi([0,2\pi])$ as $\sigma_{\mathrm{I}}=\lambda\sin\theta\cos\phi$, $\sigma_{\mathrm{II}}=\lambda\sin\theta\sin\phi$ and $\sigma_{\mathrm{III}}=\lambda\cos\theta$. The proportionality constant λ is determined based on the minimum of the set of $(\sigma_{\mathrm{I}},\sigma_{\mathrm{II}},\sigma_{\mathrm{III}})$ triplets satisfying Eq. (1) on 12 possible ⟨001⟩ {110} slip systems. This procedure is repeated for all of the angles θ and ϕ within the corresponding limits. As can be seen in Fig. 3, the yield locus generated by Eq. (1) is asymmetric unlike the Schmid Law based locus. Note that the maximum differential between two yield loci exceeds 360 MPa indicating the significance of non-glide stresses.

3. Discussion of the results

The presence of the tension–compression asymmetry for the ⟨111⟩ oriented samples points to the effect of the normal non-glide stress components, S_{11} and S_{22} (S_{33} is linearly dependent on these two components). To that end, these normal components introduce displacements in the lattice structure which are not parallel to the glide vector, **b**. Similar behavior has been also reported for pure bcc metals [31] and must be linked with the dislocation core spreading [41,43,44]. Therefore, it is surmised that the elastic lattice displacements associated with these components contribute to the CRSS values in an increasing/decreasing fashion when they are of tensile/compressive nature.

A possible explanation for the tension–compression asymmetry in the ⟨249⟩ and ⟨011⟩ oriented samples can be given based on the ratio between the non-glide and glide shear stress components S_{21}/S_{23}. In the case of the ⟨249⟩ oriented sample, the non-glide shear stress, S_{21}, under tension acts along an opposite sense to the dislocation glide force, $\mathbf{F}=(\boldsymbol{\Sigma}:\mathbf{b})\times\boldsymbol{\xi}$ where **b** and **ξ** are the slip vector and the normalized dislocation line direction chosen parallel to **b** based on the Right Hand Side-Start Finish convention [45]. On the other hand, S_{21} and **F** are directed along the same sense under compression. As the CRSS value for the ⟨249⟩ oriented sample is measured to be greater under tension than it is under compression, it is evident that the opposing effect of S_{21} (which is manifested as a narrowing of the core size) under tension increases the glide resistance. Similar analogy can be also established for the ⟨011⟩ oriented sample in which the component S_{21} facilitates/opposes the glide under tension/compression by acting in the same/opposite sense with respect to the glide force.

An important aspect of the anisotropic character of CRSS values in B2 NiTi is that the deviations from the Schmid law persist even at 293 K unlike the other bcc materials studied in the literature with the exception of transition metal intermetallics [12,17]. In B2 NiTi, the strong d Ti–p Ni and d Ti–d Ti orbital hybridizations prevail over the weak d Ni–d Ni bonding [46,47]. In the case of almost equi-atomic composition B2 NiTi, the recent positron lifetime measurements confirmed the anisotropic covalent nature of the electron density [48]. The strong non-Schmid effects experimentally observed in this study most likely originate from this strongly anisotropic bonding character present in B2 NiTi.

The generalized yield criterion proposed in Eq. (1) can be interpreted as the equivalency of a generalized stress measure to a critical yield stress, τ_{cr}^{*}. However, the free energy change associated with dislocation core spreading in B2 NiTi imposes that τ_{cr}^{*} is not equal to CRSS which is the work conjugate stress to the glide shear on ⟨001⟩ {110} [49,50]. The orientation dependency of the CRSS values in Fig. 2 is reflected on the yield locus shape in Fig. 3 by the parameters a_1 and a_3 as the relation between S_{21}/S_{23} and S_{13}/S_{23} ratios are χ angle dependent. On the other hand, the parameters a_2 and a_4 prevail on the tension and compression asymmetry linked with the change of the signs of the normal non-glide stress components. Moreover, these parameters promote the lattice glide resistance of B2 NiTi. As a result of this strengthening effect, the yield locus predicted by the Schmid law is enclosed by the yield locus predicted by Eq. (1) as can be seen in Fig. 3.

We rule out the presence of martensitic transformation (MT) in our experiments via three methods: (i) the max. measured DIC strains are much different in slip and MT cases (approx.3–3.5% versus 7% respectively). We considered an aged ⟨294⟩ orientated sample and studied MT (superelasticity) and measured strains near 7%, (ii) the strain localization planes shown in Fig. 1 do not correspond to habit plane variants in NiTi which are of

{−0.8889, −0.404, 0.2152} family. In fact, the strain localization corresponds to {011} slip planes as we expect. Finally, (iii) the EBSD results do not show MT (no local orientation change) at all and no mechanical twinning is observed for the orientations shown in the paper (for the [001] loading case mechanical twinning can occur and in that case the EBSD results clearly show the occurrence of {114} twinning [51]).

Returning to point (i) above, the high strain magnitudes in the MT (>6%) have been shown in our early experimental work [52]. Moreover, the strain evolution mechanism during deformation is also very different between MT and plastic slip cases (to study MT in single crystals, we aged the samples). The martensitic front advances until it engulfs the entire specimen in the MT case. On the other hand, in the plastic slip case (Fig. 1) the plastic strain localizes and does not traverse the specimen at all. Therefore, the resulting spatial strain distribution with time differs between the superelastic NiTi and plastically deformed NiTi. Our results conform to the plastic slip case. Finally, as stated earlier we measured via EBSD the orientations before and after deformation in solutionized case, and confirmed no change has been detected. Therefore, we emphasize that this is a study of pure plastic slip (solutionized case) and not combined MT and slip.

Finally, we note that when MT occurs in the aged case, then plastic slip and phase transformation can occur simultaneously and the plastic slip can affect the stress hysteresis and the transformation strains in an adverse manner [4]. Therefore, combined MT+ slip is also an important topic, but is outside the scope of this paper. The occurrence of non-Schmid behavior for MT was noted by Sehitoglu's group on single crystals in early work [20,53,54]. We note that the previous treatments of transformation and plasticity interaction are important, and the development of non-Schmid inspired yield criteria can be incorporated to handle to characterize complex interactions [9,55]. Such a modification is important not only in deformation studies but also in advanced models for fatigue in NiTi alloys. We acknowledge that the understanding of slip remains a current and difficult topic in SMAs [8] which has been our focus in this paper. Our study is aimed at developing a better understanding.

4. Conclusions

Following conclusions are drawn from this work on 50.8% at. Ni–NiTi alloys:

(i) The slip is activated along ⟨001⟩ {110} slip systems for all three of the ⟨111⟩, ⟨249⟩ and ⟨011⟩ oriented single crystal samples under uniaxial tension and compression loading. The single crystals facilitate the determination of the precise stress tensor components in the dislocation frame.

(ii) The onset of plastic glide does not obey Schmid law and exhibits both significant tension–compression asymmetry as well as crystal orientation dependency under uniaxial loading. The magnitude of the non-Schmid effect is substantial exceeding other bcc metals such as Fe.

(iii) The non-glide shear stress acting on glide plane in the same/opposite sense with the dislocation glide force facilitates/hardens the slip. On the other hand, the positive sense normal character non-glide stresses increase the glide resistance.

(iv) A generalized yield criterion than can encompass the corresponding non-Schmid behavior in B2 NiTi is proposed based on the applied deviatoric stress components. The work underscores the importance of modifications to the Schmid law to capture experimental results with accuracy.

Acknowledgments

The work is supported by Nyquist Chair funds. We also acknowledge the use of Frederick Seitz Materials Research Laboratories Center for Microanalysis of Materials for EBSD analyses at University of Illinois. The single crystals were grown by Prof. Yuriy Chumlyakov of Tomsk State University, Tomsk, Russia.

References

[1] R. Delville, B. Malard, J. Pilch, P. Sittner, D. Schryvers, Transmission electron microscopy investigation of dislocation slip during superelastic cycling of Ni–Ti wires, Int. J. Plast. 27 (2011) 282–297.
[2] D.M. Norfleet, P.M. Sarosi, S. Manchiraju, M.F.X. Wagner, M.D. Uchic, P.M. Anderson, M.J. Mills, Transformation-induced plasticity during pseudoelastic deformation in Ni–Ti microcrystals, Acta Mater. 57 (2009) 3549–3561.
[3] S. Miyazaki, S. Kimura, F. Takei, T. Miura, K. Otsuka, Y. Suzuki, Shape memory effect and pseudoelasticity in a Ti-Ni single crystal, Scr. Metall. 17 (1983) 1057–1062.
[4] R.F. Hamilton, H. Sehitoglu, Y. Chumlyakov, H.J. Maier, Stress dependence of the hysteresis in single crystal NiTi alloys, Acta Mater. 52 (2004) 3383.
[5] H. Sehitoglu, R. Hamilton, D. Canadinc, X. Zhang, K. Gall, I. Karaman, Y. Chumlyakov, H. Maier, Detwinning in NiTi alloys, Metall. Mater. Trans. A 34 (2003) 5–13.
[6] S. Miyazaki, T. Imai, Y. Igo, K. Otsuka, Effect of cyclic deformation on the pseudoelasticity characteristics of Ti-Ni alloys, Metall. Trans. A 17A (1986) 115–120.
[7] P. Sedmak, P. Ittner, J. Pilch, C. Curfs, Instability of cyclic superelastic deformation of NiTi investigated by synchrotron X-ray diffraction, Acta Mater. 94 (2015) 257–270.
[8] P. Chowdhury, H. Sehitoglu, A revisit to atomistic rationale for slip in shape memory alloys, Prog. Mater. Sci. 85 (2017) 1–42.
[9] S. Manchiraju, P.M. Anderson, Coupling between martensitic phase transformations and plasticity: A microstructure-based finite element model, Int. J. Plast. 26 (2010) 1508–1526.
[10] J.A. Moore, D. Frankel, R. Prasannavenkatesan, A.G. Domel, G.B. Olson, W.K. Liu, A crystal plasticity-based study of the relationship between microstructure and ultra-high-cycle fatigue life in nickel titanium alloys, Int. J. Fatigue 91 (Part 1) (2016) 183–194.
[11] E. Schmid, W. Boas, Plasticity of Crystals, A. Hughes and Co, London, 1950.
[12] M.S. Duesberry, The dislication core and plasticity, in: F.R.N. Nabarro (Ed.), Dislocations in Solids. Vol. 8, 1989, pp. 67–173.
[13] J. Christian, Some surprising features of the plastic deformation of body-centered cubic metals and alloys, Metall. Trans. A 14 (1983) 1237–1256.
[14] V. Vitek, Structure of dislocation cores in metallic materials and its impact on their plastic behaviour, Prog. Mater. Sci. 36 (1992) 1–27.
[15] M. Yamaguchi, Y. Umakoshi, Dislocations in b.c.c. metals and ordered alloys and compounds with b.c.c.-based ordered structures, in: V. Paidar, L. Lejcek (Eds.), The Structure and Properties of Crystal Defects, Elsevier, Czechoslovakia, 1983.
[16] T. Sakai, M.E. Fine, Failure of Schmid's law in Ti-Al alloys for prismatic slip, Scr. Metall. 8 (1974) 541–544.
[17] S. Alkan, H. Sehitoglu, Non-Schmid response of Fe3Al: The twin-antitwin slip asymmetry and non-glide shear stress effects, Acta Mater. 125 (2017) 550–566.
[18] M.S. Duesbery, V. Vitek, Plastic anisotropy in b.c.c. transition metals, Acta Mater. 46 (1998) 1481–1492.
[19] F. Takei, T. Miura, S. Miyazaki, S. Kimura, K. Otsuka, Y. Suzuki, Stress-induced martensitic transformation in a Ti-Ni single crystal, Scr. Metall. 17 (1983) 987–992.
[20] K. Gall, H. Sehitoglu, Y.I. Chumlyakov, I.V. Kireeva, Tension–compression asymmetry of the stress–strain response in aged single crystal and polycrystalline NiTi, Acta Mater. 47 (1999) 1203–1217.
[21] J.F. Byron, Plastic deformation of tantalum single crystals, J. Less Common Met. 14 (1968) 201–210.
[22] P.J. Sherwood, F. Guiu, H.C. Kim, P.L. Pratt, Plastic anisotropy of tantalum, niobium, and molybdenum, Can. J. Phys. 45 (1967) 1075–1089.
[23] T. Tomoyuki, Orientation dependence of work-hardening in iron single crystals, Japan. J. Appl. Phys. 8 (1969) 320.
[24] H. Saka, G. Taylor, Slip systems in a body-centred-cubic Li—Mg alloy, Phil. Mag. A 43 (1981) 1377–1392.
[25] M. Yamaguchi, Y. Umakoshi, T. Yamane, Y. Minonishi, S. Morozumi, Slip systems in an Fe-54 At. % Co alloy, Scr. Metall. 16 (1982) 607–609.
[26] S. Hanada, S. Wtanabe, T. Sate, O. Izumi, Deformation of Fe3Al0.8Si0.2 with DO3 structure, Trans. Japan Inst. Met. 22 (1981) 873–881.
[27] R. Hill, The Mathematical Theory of Plasticity, Oxford university press, 1998.
[28] R. Hill, J.R. Rice, Constitutive analysis of elastic–plastic crystals at arbitrary strain, J. Mech. Phys. Solids 20 (1972) 401–413.
[29] J.L. Bassani, K. Ito, V. Vitek, Complex macroscopic plastic flow arising from non-planar dislocation core structures, Mater. Sci. Eng. A 319–321 (2001) 97–101.
[30] R. Gröger, V. Racherla, J.L. Bassani, V. Vitek, Multiscale modeling of plastic deformation of molybdenum and tungsten: II. Yield criterion for single crystals based on atomistic studies of glide of screw dislocations, Acta Mater. 56 (2008) 5412–5425.

[31] H. Lim, C.R. Weinberger, C.C. Battaile, T.E. Buchheit, Application of generalized non-Schmid yield law to low-temperature plasticity in bcc transition metals, Modelling Simul. Mater. Sci. Eng. 21 (2013) 045015.
[32] A. Patra, T. Zhu, D.L. Mcdowell, Constitutive equations for modeling non-Schmid effects in single crystal bcc-Fe at low and ambient temperatures, Int. J. Plast. 59 (2014) 1–14.
[33] K. Taillard, P. Blanc, S. Calloch, C. Lexcellent, Phase transformation yield surface of anisotropic shape memory alloys, Mater. Sci. Eng. A 438–440 (2006) 436–440.
[34] A.F. Saleeb, S.A. Padula Ii, A. Kumar, A multi-axial, multimechanism based constitutive model for the comprehensive representation of the evolutionary response of SMAs under general thermomechanical loading conditions, Int. J. Plast. 27 (2011) 655–687.
[35] T. Ezaz, J. Wang, H. Sehitoglu, H.J. Maier, Plastic deformation of NiTi shape memory alloys, Acta Mater. 61 (2013) 67–78.
[36] N.S. Surikova, Y.I. Chumlyakov, Mechanisms of plastic deformation of the titanium nickelide single crystals, Phys. Met. Metall. 89 (2000) 196–205.
[37] T. Simon, A. Kröger, C. Somsen, A. Dlouhy, G. Eggeler, On the multiplication of dislocations during martensitic transformations in NiTi shape memory alloys, Acta Mater. 58 (2010) 1850–1860.
[38] O. Benafan, R.D. Noebe, S.A. Padula Ii, A. Garg, B. Clausen, S. Vogel, R. Vaidyanathan, Temperature dependent deformation of the B2 austenite phase of a NiTi shape memory alloy, Int. J. Plast. 51 (2013) 103–121.
[39] A.R. Pelton, G.H. Huang, P. Moine, R. Sinclair, Effects of thermal cycling on microstructure and properties in Nitinol, Mater. Sci. Eng. A 532 (2012) 130–138.
[40] E.M. Schulson, E. Teghtsoonian, Slip geometry in the body-centred cubic compound β'AuZn, Phil. Mag. 19 (1969) 155–168.
[41] M.S. Duesbery, On non-glide stresses and their influence on the screw dislocation core in body-centred cubic metals. I. The peierls stress, Proc. R. Soc. Lond. Ser. A Math. Phys. Eng. Sci. 392 (1984) 145.
[42] R. Asaro, V. Lubarda, Mechanics of Solids and Materials, Cambridge University Press, Cambridge, 2006.
[43] M. Yamaguchi, Y. Umakoshi, Core structure of ⟨100⟩ screw dislocations in b.c.c. crystals, Phys. Status Solidi (a) 31 (1975) 101–106.
[44] M.S. Duesbery, On non-glide stresses and their influence on the screw dislocation core in body-centred cubic metals II. The core structure, Proc. R. Soc. A 392 (1984) 175–197.
[45] J. Hirth, J. Lothe, Theory of Dislocations, second ed., Krieger Pub. Co, 1992.
[46] R. Eibler, J. Redinger, A. Neckel, Electronic structure, chemical bonding and spectral properties of the intermetallic compounds FeTi, CoTi and NiTi, J. Phys. F: Met. Phys. 17 (1987) 1533.
[47] G.L. Zhao, Theoretical Study of Electron-Phonon Interaction in β-Phase NiTi and Ni-Al Alloys, Physics and Astronomy. Vol. Doctor of Philosophy, Iowa State University, USA, 1992.
[48] Y.-F. Hu, W. Deng, W.E.N.B. Hao, L. Yue, L. Huang, Y.-Y. Huang, L.-Y. Xiong, Microdefects and electron densities in NiTi shape memory alloys studied by positron annihilation, Trans. Nonferr. Met. Soc. China 16 (2006) 1259–1262.
[49] J.R. Rice, Inelastic constitutive relations for solids: An internal-variable theory and its application to metal plasticity, J. Mech. Phys. Solids 19 (1971) 433–455.
[50] Q. Qin, J.L. Bassani, Non-schmid yield behavior in single crystals, J. Mech. Phys. Solids 40 (1992) 813–833.
[51] H. Sehitoglu, Y. Wu, S. Alkan, E. Ertekin, Plastic deformation of B2-NiTi – is it slip or twinning? Phil. Mag. Lett. (2017) 1–12.
[52] C. Efstathiou, H. Sehitoglu, Local transformation strain measurements in precipitated NiTi single crystals, Scr. Mater. 59 (2008) 1263–1266.
[53] K. Gall, H. Sehitoglu, Y.I. Chumlykov, I.V. Kireeva, H.J. Maier, The influence of ageing on critical transformation stress levels and martensite start temperatures in NiTi: Part II-Discussion of experimental results, Trans. ASME J. Eng. Mater. Technol. 121 (1999) 28–37.
[54] K. Gall, H. Sehitoglu, Y.I. Chumlyakov, I.V. Kireeva, H.J. Maier, The influence of ageing on critical transformation stress levels and martensite start temperatures in NiTi. I. Aged microstructure and micro-mechanical modeling, Trans. ASME J. Eng. Mater. Technol. 121 (1999) 19–27.
[55] A.W. Richards, R.A. Lebensohn, K. Bhattacharya, Interplay of martensitic phase transformation and plastic slip in polycrystals, Acta Mater. 61 (2013) 4384–4397.